Water Practice & Technology

IWA PUBLISHING



Water Practice & Technology Vol 18 No 4, 930 doi: 10.2166/wpt.2023.049

# Evaluation of the toxicity of textile effluent treated by electrocoagulation

Jéssica Elen Costa Alexandre Martins[a], Eliezer Fares Abdala Neto[a], Jefferson Pereira Ribeiro[a], Ari Clecius Alves de Lima[b], Francisco Wagner de Souza[c], André Gadelha de Oliveira[d], Carla Bastos Vidal [e,*] and Ronaldo Ferreira do Nascimento[a]

[a] Department of Analytical Chemistry and Physical Chemistry, Federal University of Ceará, Humberto Monte S/N Campus do Pici, Bloco 940, 60451-970 Fortaleza, CE, Brazil
[b] Ceará Industrial Technology Nucleus Foundation, Prof. Rômulo Proença Street, Pici, 60440-552 Fortaleza, CE, Brazil
[c] Federal Institute of Education, Science and Technology of Ceará – Campus Caucaia, Francisco Rocha Martins, S/N, Pabussu, Caucaia, CE, Brazil
[d] Center of Technological Sciences, University of Fortaleza, Av. Washington Soares, 1321, Edson Queiroz, 60881-905 Fortaleza, CE, Brazil
[e] Department of Chemistry and Biology, Federal University of Technology – Paraná, Deputado Heitor de Alencar Furtado St., Five Thousand Ecoville, 81280-340 Curitiba, PR, Brazil
*Corresponding author. E-mail: cvidal@utfpr.edu.br

CBV, 0000-0002-7688-8400

## ABSTRACT

Textile effluents are complex, making it difficult to choose an effective treatment. The textile effluent toxicity in *Lactuca sativa* after pulsed current (PC) electrocoagulation (EC) was evaluated in this study. The EC was performed using 304 stainless steel electrodes in batch mode. Parameters monitored included pH, temperature, color, and turbidity. Additionally, the process residue was subjected to energy-dispersive X-ray fluorescence (XFR) to determine the elements present. The process achieved proportional color and turbidity removal ranging from 97 to 99% and from 74 to 85%, respectively. Chemical oxygen demand (COD) and total nitrogen removal were 81 and 49%, respectively, in a 50 min time-lapse. The process generated approximately 1.7 kg of solid residue/$m^3$ treated effluent. The XFR results revealed the presence, mainly, of Fe, Cr, and Ni ions in the residue, as well as chlorine. The germination index (GI) and relative growth values showed that EC reduced effluent toxicity slightly, indicating the need for complementary treatment.

**Key words:** current density, dye removal, electrochemical process, electrocoagulation residue, germination index, *Lactuca sativa* toxicity

## HIGHLIGHTS

- A lower energy consumption electrocoagulation process by the pulsed current was studied for textile wastewater treatment.
- The color and turbidity removal were modeled under the influence of stirring rate, pulse frequency, and inter-electrode distance.
- XRF analysis to determine the electrochemical residue composition is essential for the process's understanding.

## GRAPHICAL ABSTRACT

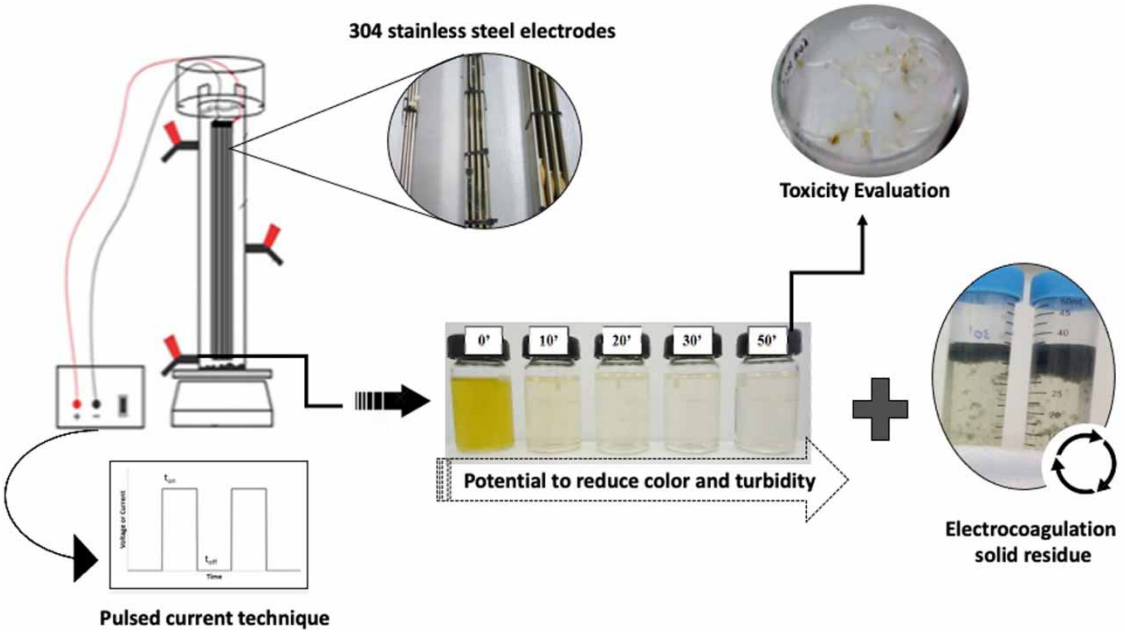


## INTRODUCTION

The complex degradation of textile processing effluents is worrying in relation to this type of effluent's characteristics. These effluents usually present high chemical oxygen demand (COD) (Ribeiro *et al.* 2014) and dye concentrations, as well as other, highly stable and toxic compounds (Azzaz *et al.* 2018), which affect the efficiency of conventional treatment, such as biological and chemical coagulation, adversely. Most dyes and their byproducts have carcinogenic potential (Ribeiro *et al.* 2014) that can cause severe risks to aquatic biota and human health. Therefore, treating these effluents effectively before discharge to water bodies is essential.

Several technologies have been studied for treating textile effluents, including ozonation (Wijannarong *et al.* 2013), sonication (Rayaroth *et al.* 2015), photocatalysis (Rosa *et al.* 2015), membrane filtration (Dasgupta *et al.* 2015), and electrocoagulation (EC) (Ribeiro *et al.* 2014).

EC is promising in treating various industrial wastewaters (Phalakornkule *et al.* 2010; Oliveira *et al.* 2020). In EC, electrode dissolution of the anode yields hydrolysis products, such as metal hydroxides, that are effective in destabilizing contaminants and/or forming particles of reduced solubility that trap pollutants (Behbahani *et al.* 2011). With the generation of coagulating agents *in situ*, the addition of chemicals and the production of excess sludge can be avoided. Mollah *et al.* (2001) reported that EC requires simple and easy-to-operate equipment, which produces an effluent with a lower concentration of total dissolved solids (TDS) than chemical treatments.

Most studies have reported using direct current (DC) in EC. However, DC can cause oxidative corrosion at the anode, as well as the formation of an oxide layer at the cathode, reducing cathode/anode current flow, and hence treatment efficiency (Khandegar & Saroha 2013). Electrode passivation also increases electrical energy consumption. The pulsed current (PC) mode has been studied in electrochemical methods in water/wastewater treatment (Lu *et al.* 2015). In addition to avoiding electrode passivation, PC has the advantage of lower energy consumption than DC (Rocha *et al.* 2018; Oliveira *et al.* 2020).

While most research involving textile effluent treatment does not address the issue of toxicity because, in some situations, even treated effluent can present high toxicity, some studies have included the use of seeds for effluent toxicity tests. Lettuce seeds (*Lactuca sativa*) in effluent, soil, or sediment are used for toxicity tests, due to the low energy reserve required for germination and their ensuing rapid growth (Dutka 1989). Tests using *L. sativa* evaluate the samples' toxic effects on germination and elongation of the root, which can show sensitivity to different compounds at different levels. In this paper, the aim was to assess color and turbidity removal, and the toxicity of the textile effluent after EC treatment by PC.

## MATERIALS AND METHODS

### Textile effluent

Duplicate samples from real textile effluent were obtained from a hammock factory in Jaguaruana-CE, Brazil. The raw effluent characteristics are shown in Table 1. The effluent is dark yellow, with a maximum absorbance peak at 400 nm (Figure 1).

**Table 1** | Physical and chemical parameters of raw effluent ($n = 2$)

| Parameter | Average value |
|---|---|
| pH | 7.4 |
| Electrical conductivity ($mS \cdot cm^{-1}$) | 12.9 |
| Turbidity (NTU) | 105.6 |
| COD ($mg\ O_2 \cdot L^{-1}$) | 848.8 |
| Absorbance (at 400 nm)[c] | 2.653 |
| Total suspended solids – TSS ($mg \cdot L^{-1}$) | 174 |
| Chloride ($g \cdot L^{-1}$) | 5.6 |

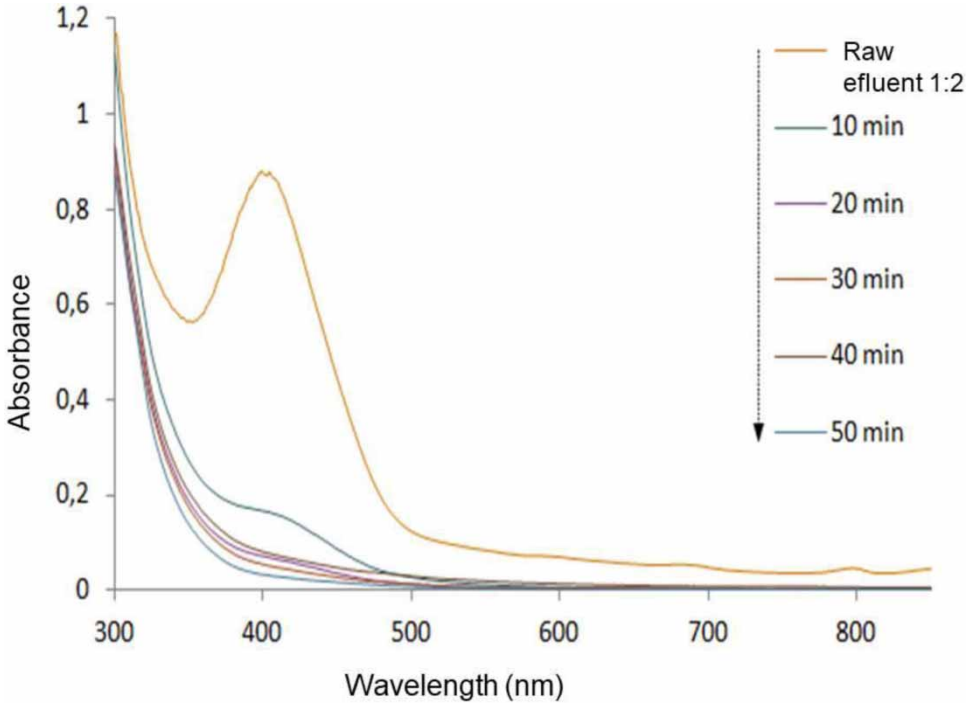


**Figure 1** | UV–Vis absorbance spectrum of the raw effluent (diluted 1:2) and samples collected after 10, 20, 30, 40, and 50 min of EC.

### EC setup

The electrolytic cell configuration was set up according to Martins *et al.* (2017). The cylindrical EC reactor (60.0 cm height and 10.0 cm I.D) was constructed in acrylic, with four parallel plate electrodes (5.0 × 40.0 × 0.3 cm) of 304 stainless steel connected by a bipolar array (total surface area 1,200 $cm^2$). A magnetic stirrer was used to mix liquids in the electrolytic medium (Tecnal TE-0851, Piracicaba/Brazil).

The PC application was carried out by an electric voltage source (Hayama® HY-1320 Plus™ 220–13.8 V, 20 A, Londrina/Brazil) connected to a homemade electric circuit (DC/PC converter). The shape of the PC technique can be observed in Figure 2. The duty cycle of 50% was obtained from $T_{on}$ and $T_{off}$ (Equation (1)). The duty cycle

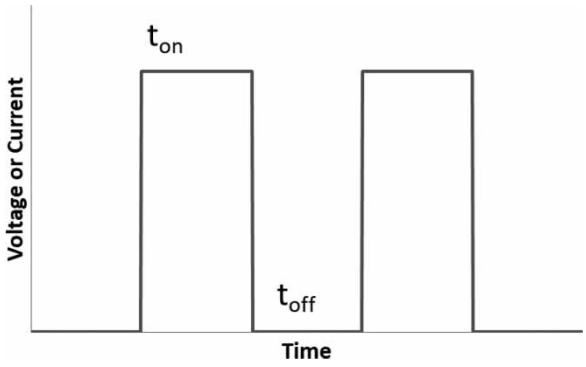


**Figure 2** | PC technique.

is defined as the ratio of the current passing in time ($T_{on}$) and the total cycle time ($T_{on} + T_{off}$), where $T_{off}$ is related to the time with no electric current. The volume of effluent used in the electrolytic reactor was 2.6 L. Samples were collected after 10, 20, 30, 40, 50, and 60 min.

$$\text{Duty cycle } (\%) = \frac{T_{on}}{T_{on} + T_{off}} \tag{1}$$

## Experimental design and data analysis

Aiming to obtain the optimum operating conditions for the process, experimental planning was carried out using statistical and mathematical resources:

- 1: Select factors (stirring rate, pulse frequency, and inter-electrode distance) and levels for the construction of the Box–Behnken design (BBD);
- 2: Obtain models from the BBD experimental results and statistical analysis;
- 3: Construct response surface graphics, demonstrating the optimal operating conditions for removing color and turbidity.

According to Aslan & Cebeci (2007), the minimum number of experiments (N) required for BBD development is defined according to the following equation (2):

$$N = 2k\,(k-1) + C_0 \tag{2}$$

where $k$ is the number of factors or independent variables and $C_0$ is the number of replicates of the central point. Three factors were selected and four repetitions of the central point were made, generating a total of 16 experiments. The responses or dependent variables, $Y_1$ and $Y_2$, were expressed as the proportions (%) of color and turbidity removal, respectively. Table 2 presents the operating conditions and average current density values for the experiments.

The experimental results enabled the development of mathematical models using the ordinary least squares method. This is used to estimate the ($\beta 0$, $\beta 1$, $\beta 2$,…, $\beta n$) coefficients used in modeling the $Y$ response, with the aim of reducing the sum of the squares of the residuals. The general form of the equation applied to the removal of color and turbidity individually is given in the following equation:

$$Y = \beta_o + \beta_1 x_1 + \beta_2 x_2 + \beta_3 x_3 + \beta_{11} x_1^2 + \beta_{22} x_2^2 + \beta_{33} x_3^2 + \beta_{12} x_1 x_2 + \beta_{13} x_1 x_3 + \beta_{23} x_2 x_3 + \varepsilon \tag{3}$$

where

- $Y$ is the dependent variable;
- $x_1$, $x_2$, $x_3$ are the coded levels of the independent variables;
- $\beta$ is the coefficients estimated by the least squares method; and,
- $\varepsilon$ is the residue that measures the experimental error.

**Table 2** | Operating conditions and average values of power and current density

| Exp. | $X_1$ (rpm) | $X_2$ (Hz) | $X_3$ (mm) | Average current density (mA cm$^{-2}$) | Color removal (%) ($Y_1$) | Turbidity removal (%) ($Y_2$) | EEC (kWh m$^{-3}$) |
|---|---|---|---|---|---|---|---|
| 1 | – | 600 | 5.5 | 0.4 | 99 | 83 | 2.5 |
| 2 | 400 | 600 | 5.5 | 0.4 | 99 | 84 | 2.4 |
| 3 | – | 2,200 | 5.5 | 0.4 | 98 | 74 | 2.5 |
| 4 | 400 | 2,200 | 5.5 | 0.4 | 98 | 82 | 2.5 |
| 5 | – | 1,400 | 1.0 | 0.5 | 99 | 81 | 3.3 |
| 6 | 400 | 1,400 | 1.0 | 0.5 | 99 | 85 | 3.3 |
| 7 | – | 1,400 | 10.0 | 0.4 | 98 | 78 | 2.3 |
| 8 | 400 | 1,400 | 10.0 | 0.4 | 98 | 80 | 2.3 |
| 9 | 200 | 600 | 1.0 | 0.5 | 99 | 88 | 3.3 |
| 10 | 200 | 2,200 | 1.0 | 0.5 | 99 | 84 | 3.3 |
| 11 | 200 | 600 | 10.0 | 0.4 | 98 | 84 | 2.3 |
| 12 | 200 | 2,200 | 10.0 | 0.4 | 98 | 82 | 2.3 |
| 13 | 200 | 1,400 | 5.5 | 0.4 | 99 | 84 | 2.5 |
| 14 | 200 | 1,400 | 5.5 | 0.4 | 99 | 83 | 2.5 |
| 15 | 200 | 1,400 | 5.5 | 0.4 | 99 | 84 | 2.5 |
| 16 | 200 | 1,400 | 5.5 | 0.4 | 99 | 84 | 2.5 |

Exp, experiment; $X_1$, stirring rate; $X_2$, pulse frequency; and $X_3$, inter-electrodes distance.

The validity of the assumption of normality of the residuals was evaluated using least square estimators and regression analysis was also based on which errors followed a normal distribution. The experimental data were processed using R software (R Development Core Team 2014).

## Analytical methods

Before color and turbidity analysis, the samples were left for 1 h to allow floc particles (suspended solids) to settle. Turbidity analysis was performed using a portable turbidimeter (Hach, 2100P). Color analysis was performed on the supernatants after separating the suspended solids by centrifugation at 4,000 rpm for 5 min. Absorbance was measured by spectrophotometry (Shimadzu, UV-1800) at 400 nm and the UV–Vis spectral for color removal evaluation. Sample pH was measured immediately after sampling using a pH meter (Tecnal Tec 5). A thermometer 20 cm from the reactor top measured the temperature *in situ*.

The electrical energy consumption (EEC) per unit volume of treated effluent (kWh m$^{-3}$) was obtained using the following equation:

$$\text{EEC (kWh m}^{-3}) = \frac{Tit}{1,000\text{V}} \tag{4}$$

where $T$ is the applied tension (V), $i$ is the electrical current (A), $t$ is the duration of the experiment (h), and $V$ is the volume of solution (m$^3$).

## Toxicity tests

The tests were conducted using lettuce seeds (*L. sativa*), which were exposed to the different concentrations (1, 10, 25, 75, and 100% v/v) of the textile effluent before and after EC, within the optimum operating conditions (Martins *et al.* 2017), to evaluate both lethal effects through non-germination and sublethal impacts through the development of radicles. The seeds were seeded using Petri dishes ($\varnothing = 9.5$ cm) and duplicated for each concentration tested. Each plate was prepared by placing a filter paper in the base, to which 4 mL of effluent sample was added, and, with the aid of forceps, 20 seeds were disposed of equidistantly.

After this, the plates were closed to prevent moisture loss, covered in dark paper for protection against light, and conditioned at 22 ± 2 °C for 120 h (EPA 1989). For each test, distilled water was used as a control, considering acceptability criteria: seed germination ≥90% and root length variability ≤30%. Sensitivity tests were performed with sodium chloride (NaCl), at 9.21 g–NaCl L$^{-1}$ concentration, representing the positive control.

Dilutions were also made to give 10, 25, and 50% (v/v) concentrations, following the same procedure as the sample tests.

At the end of exposure, the number of seeds that germinated normally, considering as criteria the visible appearance of the radicle and measuring their lengths in each of the seedlings quantified. From the germination data, radicle length was calculated using both the relative growth index (RGI) and the germination index (GI), via the following equations (Alvarenga *et al.* 2007).

$$\mathrm{RGI} = \mathrm{ARS}/\mathrm{ARC} \tag{5}$$

$$\mathrm{GI} = \mathrm{RGI} \times (\mathrm{AGS}/\mathrm{AGC}) \times 100 \tag{6}$$

ARS and ARC are the average radicular lengths in the sample and negative control, respectively, and AGS and AGC are the average numbers of germinated seeds in the sample and negative control, respectively. RGI values were classified into three categories according to the toxicity effects observed (Young *et al.* 2012):

(a) Inhibition of root elongation (I): $0 < x < 0.8$
(b) No significant effects (NSE): $0.8 \leq x \geq 1.2$
(c) Stimulation of root elongation (S): $x > 1.2$

where $x$ is the value obtained for RGI.

### Analysis of the solid residue

After total sedimentation, the residue (scum and sludge) generated by EC under optimum operating conditions (Martins *et al.* 2017) was collected and conditioned in a drying oven at 105 °C until a constant weight was attained. The dry mass was subjected to energy-dispersive X-ray fluorescence (XFR) analysis (Rigaku-ZSX Mini II) for elemental identification.

## RESULTS AND DISCUSSION

### Temperature, pH, turbidity, and color monitoring

The temperature values monitored throughout the EC studies are presented in Figure 3. In all 16 experiments, the temperature increased with a maximum variation of around 6 °C (final temperature = 32.3 °C, Experiment 12) and a minimum of 3 °C (final 29 °C, Experiments 2 and 16). The Joule effect can explain these increases during EC. According to Daneshvar *et al.* (2006), the solution's temperature increases before EC contributed to the removal efficiency caused by the movement of the ions, producing collisions with the coagulant formed. Chen (2004) reported that this temperature increase provides higher conductivity and consequently, lower energy consumption.

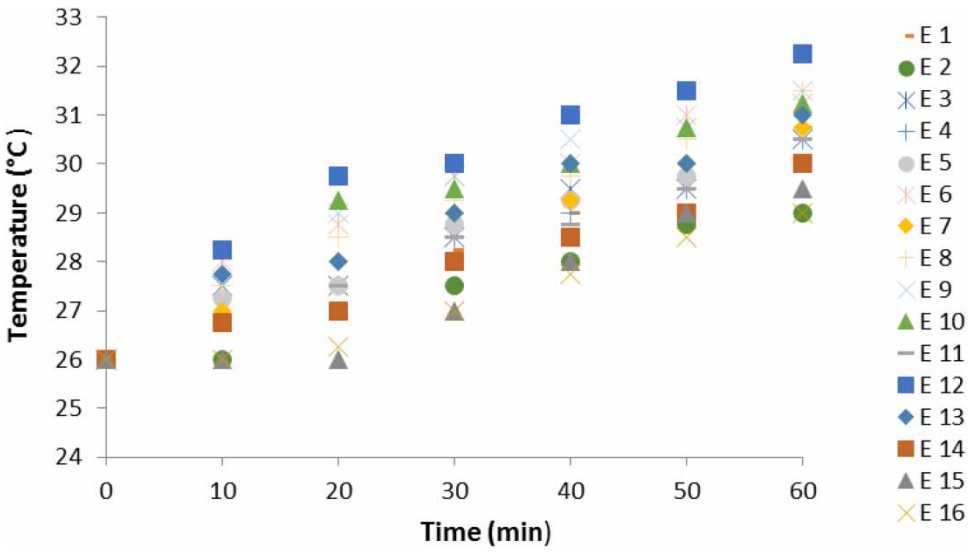


**Figure 3** | Temperature behavior over the EC period.

Electrical conductivity values showed slight increases at the ends of the experiments, with the most significant variation in Experiment 13 (710 $\mu S \cdot cm^{-1}$) and the lowest in Experiment 15 (210 $\mu S \cdot cm^{-1}$) (Figure 4). The increase in conductivity may be related to the increase in temperature, since the temperature rise generally increases the solution's conductivity because the average kinetic energy of the ions increases and the solvent's viscosity decreases, so the ions can move faster and improve conductivity.

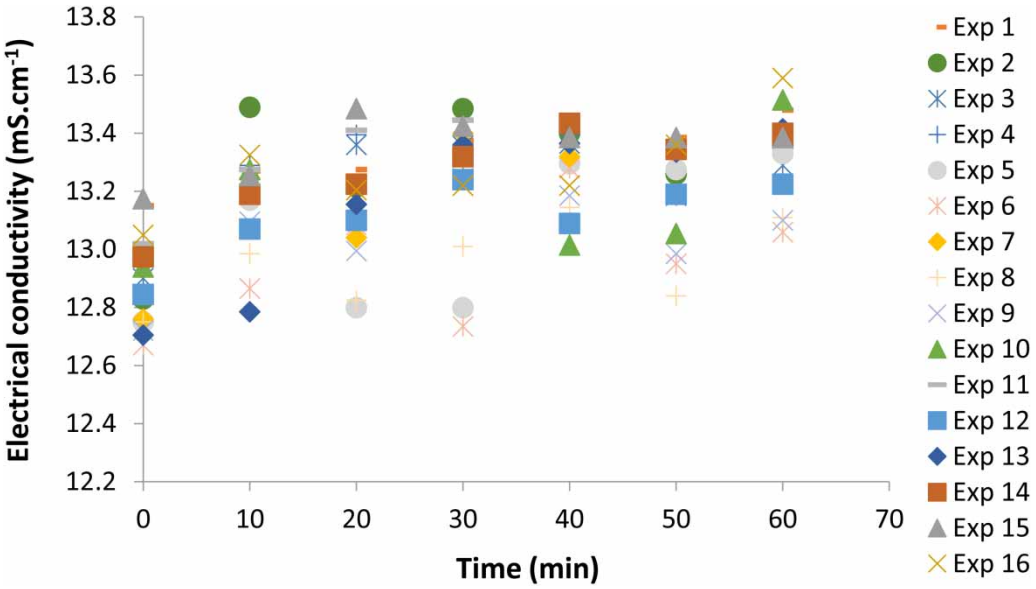


**Figure 4** | Conductivity behavior over the EC period.

In EC treatment, pH is essential in determining treatment efficiency. As shown in Figure 5, pH increased throughout EC in all experiments, with the most significant variation in the first 10 min. Experiment 5 obtained the highest pH (11.06) at the end of the experiment, possibly as it involved the highest current density. This increase in pH during EC can be explained by water reduction at the cathode (Equation (7)) (Verma 2017). The pH increase was also observed during EC in other studies using stainless steel electrodes to treat textile

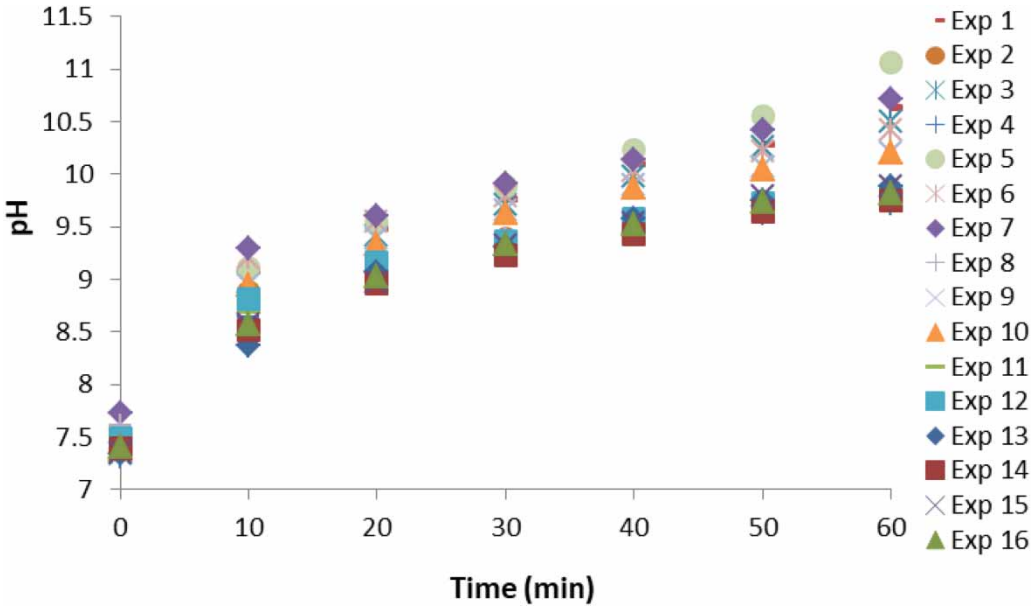


**Figure 5** | pH evolution during EC treatment for each experiment.

effluents (Bener *et al.* 2019)

$$2H_2O_{(l)} + 2e^- \rightarrow H_{2(g)} + 2OH^-_{(aq)} \quad (7)$$

Electrochemical reactions at the iron anodes can generate ferrous or ferric cations (Equations (8) and (9).

$$Fe \rightarrow Fe^{2+} + 2e^- \quad (8)$$

$$Fe \rightarrow Fe^{3+} + 3e^- \quad (9)$$

The $Fe^{3+}$ species is the one desired since $Fe^{3+}$ ions can undergo hydrolysis generating $Fe(OH)^{2+}$, $Fe(OH)_2^+$, $Fe(OH)_3$, and $Fe(OH)_4$ (Figure 6). The initial pH of the EC was around 7.0 with the major species in the medium being $Fe(OH)_2^+$ and $Fe(OH)_3$. After 10 min and throughout the process, the pH increased (approximately 8.5–9.5), favoring the $Fe(OH)_3$ and $Fe(OH)_4^-$ species. The formation of $Fe(OH)_3$ provides good absorption capacity for the pollutant and, when present, the solution is yellowish (Akyol 2012). Nasrullah *et al.* (2020) verified the formation of larger flocs in their study due to $Fe(OH)_3$. $Fe(OH)_4^-$ is not desired because its coagulation efficiency is lower.

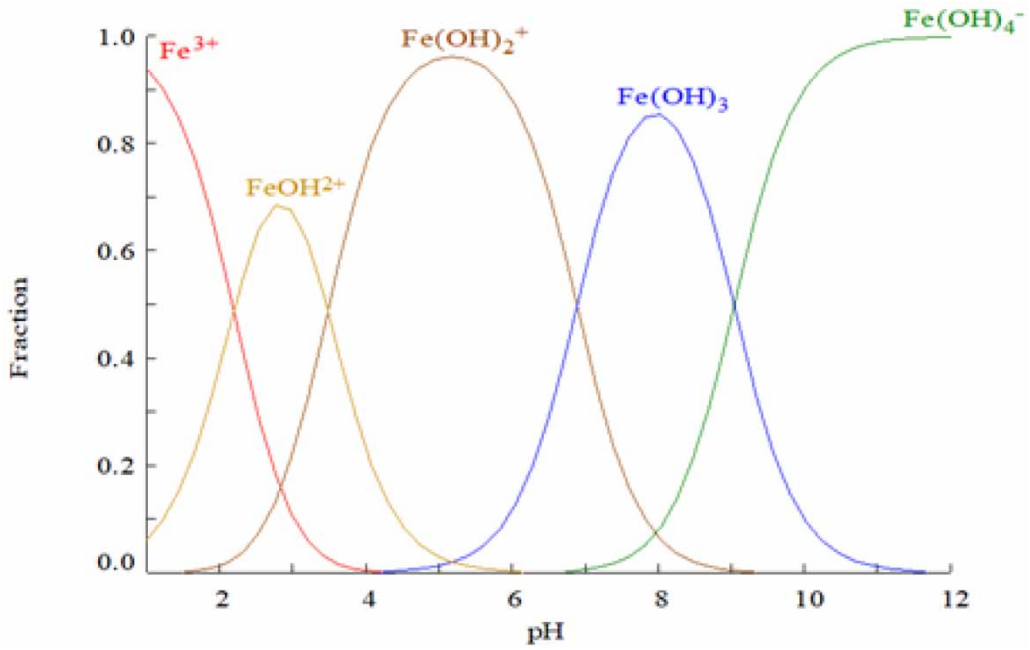


**Figure 6** | Molar fractions of iron species dissolved in equilibrium with amorphous hydroxide, 25 °C.

As shown in Figure 7, absorbance decreased throughout all EC experiments, reaching removal percentages above 97% in only 20 min of operation. At the end of the process, the results of color removal were remarkably close, varying between 97.8 and 99.1%. A possible explanation for these results is the small variation between current densities (0.359–0.523 mA/cm$^2$, Table 2). The highest current densities achieved the best color removal (Table 2). Current density is one of the most important parameters for controlling the reaction rate, mainly by determining the amount of coagulant released into the solution. However, higher current density values may not improve the process due to the possibility of electrode polarization (Oliveira *et al.* 2020).

Turbidity removal proportions above 95% were achieved within 20 min. However, as shown in Figure 8, after 30 min of EC, turbidity tends to increase slightly. After 60 min of EC, the lowest turbidity removal was 74% (final value of 26.8 NTU, Experiment 3), and the highest was 91% (10.7 NTU, Experiment 9), Table 2. In color and turbidity removal, Experiment 9 achieved the best removals since it had the highest current density (0.512 mA cm$^{-2}$), Table 2.

In addition to color and turbidity removals, EEC must be quantified, as it will indicate the cost of treatment. EEC was calculated for the experiments, Table 2, and the values obtained were between 2.29 and 3.33 kWh m$^{-3}$.

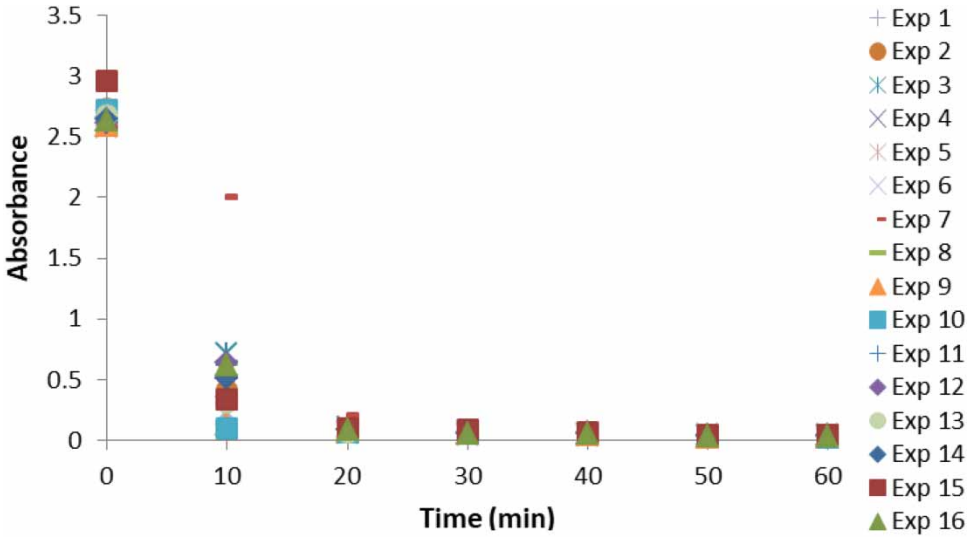


**Figure 7** | Absorbance removal over the EC period. Absorbance at $\lambda = 400$ nm.

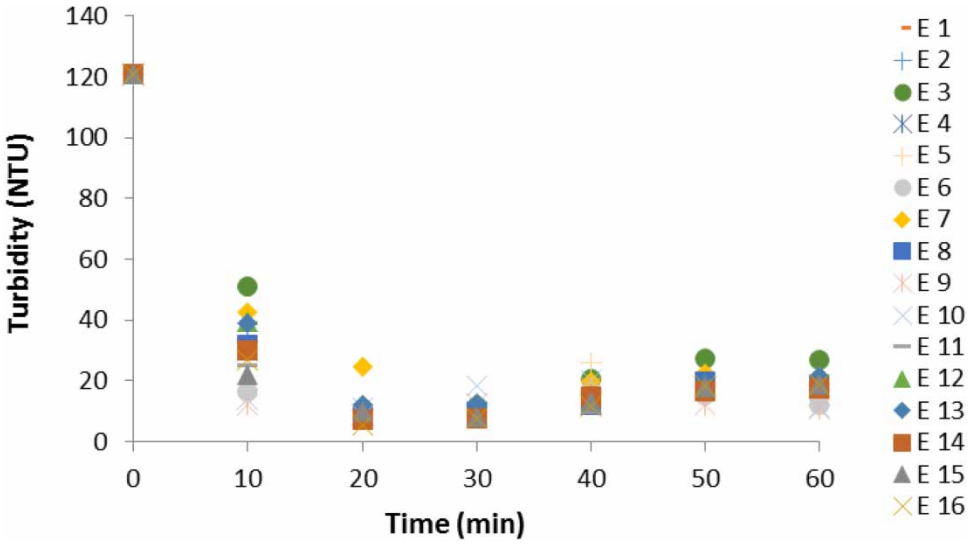


**Figure 8** | Turbidity removal throughout EC treatment.

## Statistical modeling and analysis

Table 3 shows the mathematical model coefficients estimated by the software, the coefficients' standard deviations, the respective *t*-Student values, and the significance of each regression coefficient through the '*p*' value. Statistically significant coefficients, considering a 95% confidence interval ($p < 0.05$), are highlighted in bold.

Models were obtained only with the statistically significant plots by the significance probability test ($p < 0.05$), which relates the response variables to the independent variables presented below, according to Equations (10) and (11). $X_1$, $X_2$, and $X_3$ are the values of the independent variables, agitation speed, pulse frequency, and inter-electrode distance, respectively. The coefficient values for each installment were rounded to the fourth decimal place.

$$\text{Color removal (\%)} = 98.6225 - 0.1638\,X_2 - \ 0.3813\,X_3 - \ 0.2263\,X_1^2 - 0.2025\,X_1X_3 \tag{10}$$

$$\text{Turbidity removal (\%)} = 83.5088 + 1.8025X_1 - 2.1306X_2 - 1.8319X_3 - 3.0325X_1^2 + 1.4875\,X_1X_2 \tag{11}$$

**Table 3** | Coefficients of linear regression, coefficient standard deviations, *t*-values, and probability of model coefficients' statistical significance (*p*) regarding color and turbidity removal

| Response | Factor | Coefficient | Standard deviation | *t*-value | *p*-Value |
|---|---|---|---|---|---|
| Color | Intercept | 98.62250 | 0.077956 | 1,265.1104 | $<2.2 \times 10^{-16}$ |
| | $X_1$ | 0.0325 | 0.055123 | 0.5896 | 0.576976 |
| | $X_2$ | − 0.16375 | 0.055123 | − 2.9706 | 0.024937 |
| | $X_3$ | − 0.38125 | 0.055123 | − 6.9164 | 0.000452 |
| | $X_1$:$X_2$ | −0.08 | 0.077956 | −1.0262 | 0.344367 |
| | $X_1$:$X_3$ | − 0.2025 | 0.077956 | − 2.5976 | 0.040792 |
| | $X_2$:$X_3$ | 0.0175 | 0.077956 | 0.2245 | 0.829828 |
| | $X_1^2$ | − 0.22625 | 0.077956 | − 2.9023 | 0.027253 |
| | $X_2^2$ | 0.04875 | 0.077956 | 0.6254 | 0.554762 |
| | $X_3^2$ | −0.01125 | 0.077956 | −0.1443 | 0.889979 |
| Turbidity | Intercept | 83.50875 | 0.43149 | 193.5359 | $1{,}284 \times 10^{-12}$ |
| | $X_1$ | 1.80250 | 0.30511 | 5.9077 | 0.0010461 |
| | $X_2$ | − 2.13062 | 0.30511 | − 6.9832 | 0.0004291 |
| | $X_3$ | − 1.83188 | 0.30511 | − 6.0040 | 0.0009612 |
| | $X_1$:$X_2$ | 1.48750 | 0.43149 | 3.4474 | 0.013677 |
| | $X_1$:$X_3$ | −0.22000 | 0.43149 | −0.5099 | 0.6283545 |
| | $X_2$:$X_3$ | 0.42125 | 0.43149 | 0.9763 | 0.3666344 |
| | $X_1^2$ | − 3.0325 | 0.43149 | − 7.0280 | 0.0004144 |
| | $X_2^2$ | 0.18625 | 0.43149 | 0.4316 | 0.6810792 |
| | $X_3^2$ | 0.48875 | 0.43149 | 1.1327 | 0.3005640 |

Positive coefficient values indicate an increase in the response value when the variable moves toward its maximum studied level. At the same time, negative values indicate an effect of increased response when the variable moves toward its minimum level. With respect to interactions, positive values indicate that the response will increase if the two variables are moving toward the same level, lower or higher, and negative values indicate an increase in the response if the variables are moving in opposite directions, that is, one variable moves toward the upper level and the other toward the lower level.

As seen in Table 3, the three independent variables were significant in some way (in linear, quadratic, or interaction terms) for the removal of color and turbidity. However, for color removal, the inter-electrode distance in the linear term ($X_3$) stood out compared to the other variables ('*p*' values $= 4.52 \times 10^{-4}$), influencing the removal of both parameters inversely (the higher the level, the lower the removal efficiency).

Regarding turbidity, the frequency of the pulses ($X_2$) and the inter-electrode distance ($X_3$) were highlighted, the linear term with '*p*' values equal to 4.291 and $9.612 \times 10^{-4}$, respectively, and the agitation speed in the quadratic term ($X_1^2$), with a '*p*' value equal to ($4.144 \times 10^{-4}$). The coefficients in these three cases were negative, indicating that turbidity removal will tend to decrease when the $X_2$, $X_3$, and $X_1^2$ values increase.

Figure 9 illustrates the *Q*–*Q* plot graphs, which allow the inspection of normality by comparing the accumulated frequency of standardized residues with the normal curve for each response variable. Figure 9 indicates that the errors are normally distributed since most of the points are located approximately along the line,

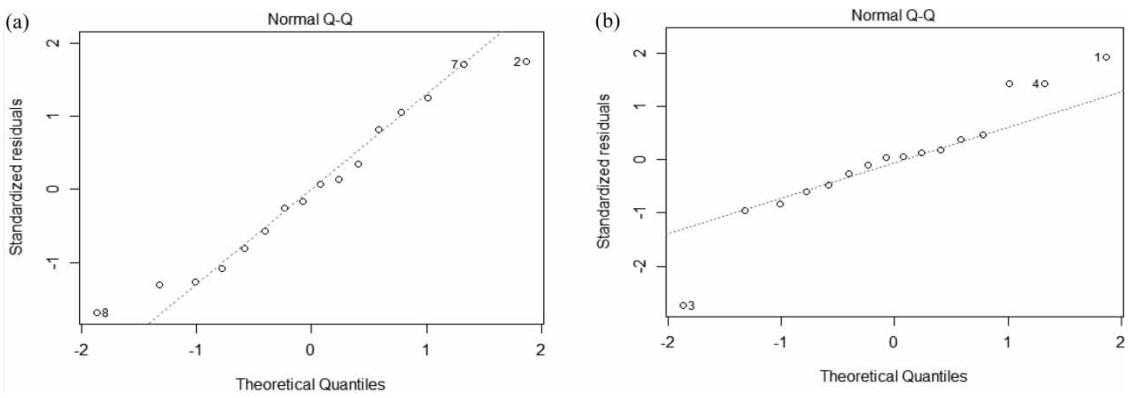


**Figure 9** | Plots of the normal probability of the residuals for the response variables: removal of (a) color; (b) turbidity.

implying the reliability of the experimental points obtained. The calculated coefficient of determination ($R^2$) represents how much of the experimental variance can be explained by the proposed model. In this case, $R^2$ was around for color at 81 and 92% for turbidity.

### Analysis of response surfaces

The pulse frequencies were fixed at their midpoint value (1,400 Hz) and the variables stirring rate and inter-electrode distance were compared with the response surface. The color and turbidity removals were intensified when the inter-electrode distance decreased to 1 mm, with stirring rates in the ranges of 200–400 rpm and 200–350 rpm for color and turbidity, respectively (Figure 10(a) and 10(b)). In Figure 10(c) and 10(d), the inter-electrode distance was kept constant at its midpoint value (5.5 mm).

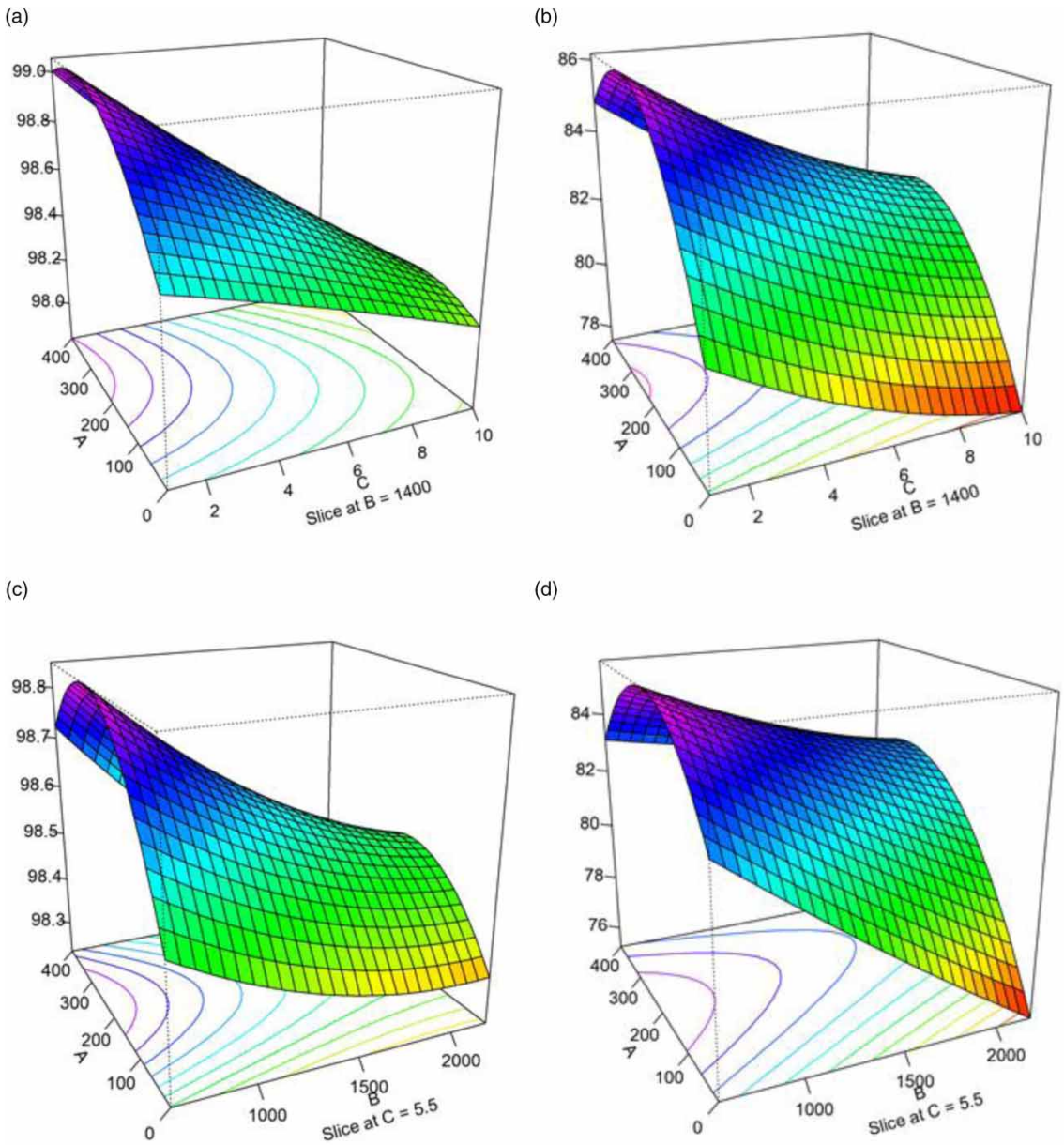


**Figure 10** | Response surface for (a) Color removal (%) vs. stirring rate (A) and inter-electrodes distance (C); (b) Turbidity removal (%) vs. stirring rate (A) and inter-electrodes distance (C); (c) Color removal (%) vs. *x* stirring rate (A) *x* pulse frequency (B); and (d) Turbidity removal (%) vs. *x* stirring rate (A) *x* pulse frequency (B).

Removals (%) tend to increase when the pulse frequency is reduced to the lowest level studied (600 Hz), the stirring rates were between 150 and 350 rpm, 100 and 320 rpm, for color and turbidity, respectively.

It was observed that decreases to the lower levels of pulse frequency and inter-electrode distance used favored increases in color and turbidity removal efficiency (Figure 11(a) and 11(b)).

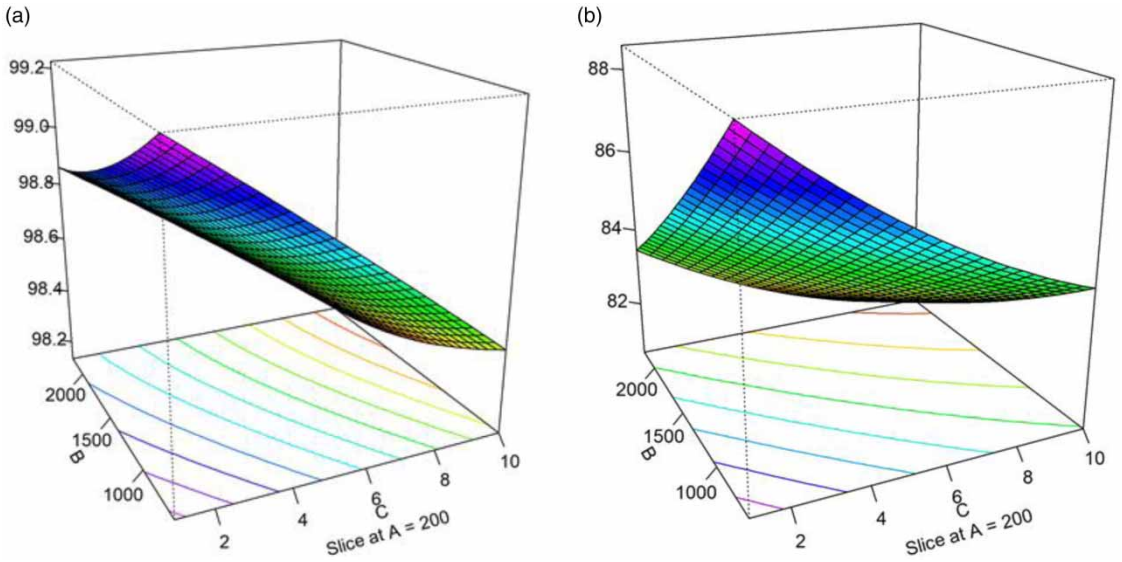


**Figure 11** | Response surface for (a) Color removal (%) vs. *x* pulse frequency (B) *x* inter-electrode distance (C) and (b) Turbidity removal (%) vs. *x* pulse frequency (B) *x* inter-electrode distance (C).

Table 4 shows the optimal values of the operating variables and the removal proportions calculated from the response surface methodology for color and turbidity.

**Table 4** | Optimal values of the independent variables

| Parameter | Stirring rate (rpm) | Pulse frequency (Hz) | Inter-electrode distance (mm) | Removal (%) |
|---|---|---|---|---|
| Color | 250.4 | 1,009.6 | 1.74 | 99.08 |
| Turbidity | 219.8 | 871.2 | 2.15 | 86.91 |

The optimization study showed that for color and turbidity removal:

(a) The optimum stirring rate was close to the midpoint studied (200 rpm), indicating that, at lower stirring rates, ion mobility within the reactor may not favor floc formation. At the highest stirring rates, however, flocs can collide with one another due to the high turbulence (Modirshahla *et al.* 2008), being able to provide larger numbers of smaller suspended and dissolved particles in the medium, increasing turbidity and color levels.

(b) The optimum inter-electrode distance was closer to the lowest level studied (1 mm); similar results were also found by Modirshahla *et al.* (2007). Low inter-electrode distance might make electron flow easier (as shown by the higher current densities, Table 2), increasing the amount of coagulating agent.

(c) The optimum pulse frequencies were around 1,000 Hz (between the lowest and midpoint levels). The exact frequency was found by Lu *et al.* (2015) and Shu *et al.* (2016) when studying sulfide removal in sewage and manganese and ammoniacal-nitrogen removals in wastewater, respectively. Xu *et al.* (2017) found 5,000 Hz for zinc and manganese removal efficiencies in smelting wastewater. The pulse frequency affects the ion migration rate and reduces the electrode's concentration polarization. Still, the mass transfer may be limited by higher pulse frequencies (Shu *et al.* 2016).

### Effluent physico-chemical characterization

Following optimization, a sample of raw water was submitted to EC treatment using a 200 rpm stirring rate, 1,000 Hz frequency, and 1 mm inter-electrode distance. Process efficiency was evaluated using parameters including pH, conductivity, turbidity, COD, color, total suspended solids (TSS), sulfate, chloride, etc. (Martins *et al.* 2017).

Removal was satisfactory for COD, turbidity, color and sulfate, reaching 81, 86, 99, and 99%, respectively. The process reached 46% removal of TSS (Martins *et al.* 2017). It is known that EC is not efficient for chloride removal.

### Toxicity tests

Treated effluent obtained under optimal conditions was used in the toxicity tests.

#### Seed sensitivity test

The seeds were exposed to different concentrations of the stressing agent (NaCl) to verify their sensitivity. The results were expressed as mean root growth (cm), RGI, and GI (Table 5 and Figure 12).

**Table 5** | Data from *L. sativa* seed sensitivity test

| NaCl dilution (% v/v) | Average radicle length (cm) | SD | CV (%) | RGI | GI (%) |
|---|---|---|---|---|---|
| 10 | 1.55 | 0.20 | 13 | 0.73 $I^a$ | 69.19 |
| 25 | 1.37 | 0.32 | 22 | 0.65 $I$ | 61.12 |
| 50 | 1.20 | 0.27 | 22 | 0.57 $I$ | 53.54 |

[a]Inhibition of radicle growth

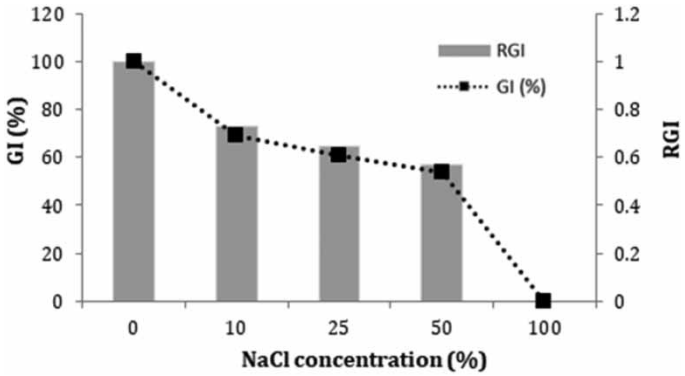


**Figure 12** | RGI and GI% of *L. sativa* seeds as a function of NaCl concentration (%) in the sensitivity assay.

The results proved the seeds' sensitivity to NaCl, with a concentration-dependent toxicity response in which both seed RGI and GI (%) decreased with increasing NaCl concentration, causing radicle growth inhibition at a concentration of only 10% (v/v). When 100% (v/v) NaCl concentration was tested, complete inhibition of seed germination occurred.

#### Toxicity tests with effluent samples

The toxicity test results with *L. sativa* were acceptable (seed GI = 100% and root length variability = 18%) according to the criteria established by the negative control. Using raw effluent at 100% (v/v) concentration, total inhibition of seed germination was observed. The toxicity test results for raw and EC-treated effluent (under optimal conditions 200 rpm, 1,000 Hz, and 1.0 mm) are presented in Table 6 and Figure 13.

Table 6 and Figure 13 show that as the effluent concentrations increased, both RGI and GI (%) decreased. The full concentration of the treated effluent also reached a low GI (0.72%). Both raw and treated effluent inhibited radicle growth from a concentration of about 50% (v/v).

**Table 6** | Toxicity test data for *L. sativa* seeds as a function of raw and EC-treated effluent concentrations

| | Effluent concentration (v/v/%) | Average radicle length (cm) | SD | CV | RGI | GI (%) |
|---|---|---|---|---|---|---|
| Raw effluent | 1 | 1.90 | 0.36 | 0.19 | 0.91 NSE[a] | 77.35 |
| | 10 | 1.81 | 0.4 | 0.22 | 0.87 NSE | 76.13 |
| | 50 | 1.53 | 0.22 | 0.14 | 0.73 *I* | 54.94 |
| | 75 | 0.86 | 0.18 | 0.21 | 0.41 *I* | 39.22 |
| | 100 | – | – | – | – | – |
| Treated effluent | 1 | 2.38 | 0.35 | 0.15 | 1.12 NSE | 118.26 |
| | 10 | 1.96 | 0.26 | 0.13 | 0.95 NSE | 87.63 |
| | 50 | 1.65 | 0.37 | 0.22 | 0.79 *I* | 68.13 |
| | 75 | 1.19 | 0.25 | 0.21 | 0.57 *I* | 42.70 |
| | 100 | 0.60 | – | – | 0.29 *I* | 0.72 |

[a]Toxicity categories (*I*), inhibition of the root elongation; NSE, no significant effects.

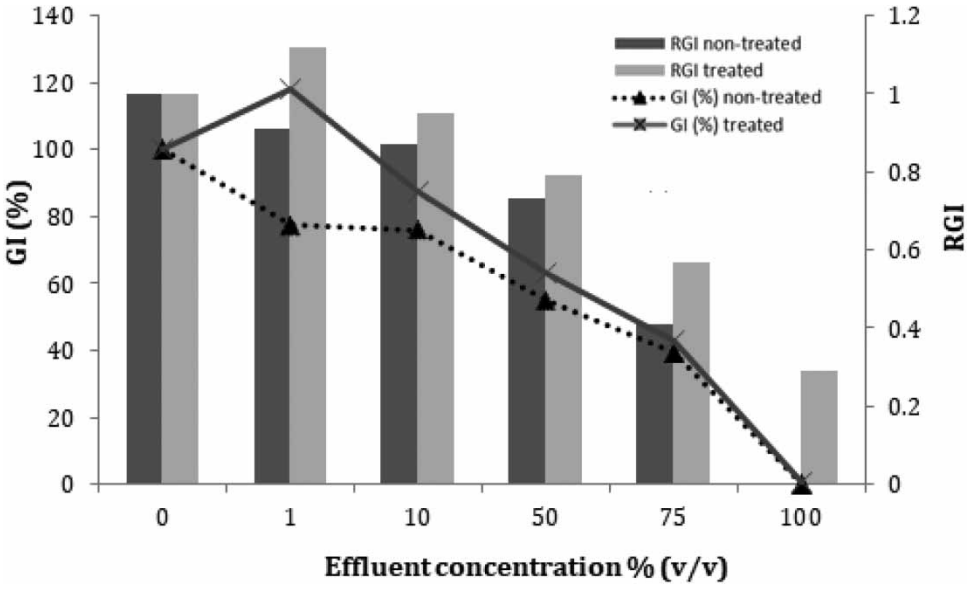


**Figure 13** | RGI and GI of *L. sativa* seeds as a function of effluent concentration (raw and EC-treated).

Due to the textile effluent's complexity, i.e., the variety of chemicals used, including dyes from different grades, synthetic gums, salts, surfactants, etc., it is difficult to identify the leading cause of toxicity. It is believed that one cause of the treated effluent's remaining toxicity is the NaCl it contains, as neither the chloride concentration nor the electrical conductivity decreased during treatment (Table 4).

In the seed sensitivity test, which considered the approximate concentration of NaCl in the raw effluent, positive effects of *L. sativa* on germination and root growth inhibition were presented against this salt, and similar results were found by Young *et al.* (2012).

Although the total nitrogen concentration decreased after EC (Table 2), toxic nitrogen species may have been formed from the oxidative process, as shown by the decrease in oxidation–reduction potential (ORP) (Table 4). This phenomenon is also observed by Palácio *et al.* (2009) who used iron electrodes in the EC treatment of textile dye effluent.

## Residue analysis

The residue generated during EC was weighed and a total mass of 4.41 g was reported. As the treated effluent volume was 2.60 L, EC treatment generated approximately 1.7 kg of solid residue/$m^3$ treated effluent, which was subjected to energy-dispersive XFR analysis – Table 7.

**Table 7** | Elemental analysis of EC treatment residue

| Element | Mass (%) |
|---|---|
| Fe | 67.11 |
| Cr | 14.91 |
| Ni | 9.20 |
| Cl | 5.39 |
| Mn | 0.96 |
| S | 0.78 |
| Ca | 0.70 |
| Al | 0.37 |
| Cu | 0.18 |
| K | 0.18 |
| Mo | 0.16 |

Iron, chromium, nickel, manganese, and sulfur were expected in the residue because they were components of the 304 stainless steel electrodes used. The three main electrode components (Fe, Cr, and Ni) were also those found in the greatest proportions in the residue mass. The presence of chlorine in the residue is also relevant because of the high concentration of chloride found in the effluent.

## CONCLUSIONS

EC by PC using stainless steel electrodes was investigated in relation to textile wastewater in this study, leading to four conclusions:

- The process's color and turbidity removal efficiencies were 98–99% and 74–85%, respectively.
- Statistical modeling and response surface data defined the optimum values for stirring rate, inter-electrode distance, and pulse frequency. The optimum stirring rate was close to 200 rpm. The best inter-electrode space was 1 mm and the optimum pulse frequency was 1,000 Hz.
- Based on the optimal independent variable values, toxicity tests with *L. sativa* seeds were a simple and efficient tool to evaluate the quality of EC-treated effluent. These tests with *L. sativa* showed that the EC-treated effluent was still highly toxic, probably due to the high NaCl concentration remaining. This indicates that EC could form part of an effluent treatment system, but it is not recommended that it be used alone.
- The solid residue generated had significant contents of Fe, Cr, Ni, and Cl.

## DATA AVAILABILITY STATEMENT

All relevant data are included in the paper or its Supplementary Information.

## CONFLICT OF INTEREST

The authors declare there is no conflict.

## REFERENCES

Akyol, A. 2012 Treatment of paint manufacturing wastewater by electrocoagulation. *Desalination* **285**, 91–99.

Alvarenga, P., Palma, P., Gonçalves, A. P., Fernandes, R. M., Cunha-Queda, A. C., Duarte, E. & Vallini, G. 2007 Evaluation of chemical and ecotoxicological characteristics of biodegradable organic residues for application to agricultural land. *Environment International* **33**(4), 505–513.

Aslan, N. & Cebeci, Y. 2007 Application of Box-Behnken design and response surface methodology for modeling of some Turkish coals. *Fuel* **86**(1–2), 90–97.

Azzaz, A. A., Assadi, A. A., Jellali, S., Bouzaza, A. K., Wolbert, D., Rtimi, S. & Bousselmi, L. 2018 Discoloration of simulated textile effluent in continuous photoreactor using immobilized titanium dioxide: effect of zinc and sodium chloride. *Journal of Photochemistry and Photobiology A: Chemistry* **358**, 111–120.

Behbahani, M., Moghaddam, M. R. A. & Arami, M. 2011 Techno-economical evaluation of fluoride removal by electrocoagulation process: optimization through response surface methodology. *Desalination* **271**(1–3), 209–218.

Bener, S., Bulca, Ö., Palas, B., Tekin, G., Atalay, S. & Ersöz, G. 2019 Electrocoagulation process for the treatment of real textile wastewater: effect of operative conditions on the organic carbon removal and kinetic study. *Process Safety and Environmental Protection* **129**, 47–54.

Chen, G. 2004 Electrochemical technologies in wastewater treatment. *Separation and Purification Technology* **38**(1), 11–41.

Daneshvar, N., Oladegaragoze, A. & Djafarzadeh, N. 2006 Decolorization of basic dye solutions by electrocoagulation: an investigation of the effect of operational parameters. *Journal of Hazardous Materials* **129**(1–3), 116–122.

Dasgupta, J., Sikder, J., Chakraborty, S., Curcio, S. & Drioli, E. 2015 Remediation of textile effluents by membrane based treatment techniques: a state of the art review. *Journal of Environmental Management.* **147**, 55–72.

Dutka, B. J. 1989 *Methods for Microbiological and Toxicological Analysis of Waters, Wastewaters and Sediments*. National Water Research Institute (NWRI), Canada Centre of Inland Water, Ontario, Canada.

EPA 1989 *Protocols for Short Term Toxicity Screening of Hazardous Waste Sites. A.8.7. Lettuce Root Elongation (Lactuca sativa). EPA/600/3-88/029*. National Service Center for Environmental Publications, Environmental Protection Agency, Chicago, USA.

Khandegar, V. & Saroha, A. K. 2013 Electrocoagulation for the treatment of textile industry effluent – a review. *Journal of Environmental Management* **128**, 949–963.

Lu, Z., Tang, J., Mendoza, M. L., Chang, D., Cai, L. & Zhang, L. 2015 Electrochemical decrease of sulfide in sewage by pulsed power supply. *Journal of Electroanalytical Chemistry* **745**, 37–43.

Martins, J. E. C. A., Abdala Neto, E. F., Lima, A. C. A., Ribeiro, J. P., Maia, F. E. F. & Nascimento, R. F. 2017 Box-Behnken design for COD removal of textile wastewater using electrocoagulation with pulsed DC. *Engenharia Sanitaria E Ambiental* **22**(6), 1055–1064.

Modirshahla, N., Behnajady, M. A. & Kooshaiian, S. 2007 Investigation of the effect of different electrode connections on the removal efficiency of Tartrazine from aqueous solutions by electrocoagulation. *Dyes and Pigments* **74**(2), 249–257.

Modirshahla, N., Behnajady, M. A. & Mohammadi-Aghdam, S. 2008 Investigation of the effect of different electrodes and their connections on the removal efficiency of 4-nitrophenol from aqueous solution by electrocoagulation. *Journal of Hazardous Materials* **154**(1–3), 778–786.

Mollah, M. Y. A., Schennach, R., Parga, J. P. & Cocke, D. L. 2001 Electrocoagulation (EC) – science and applications. *Journal of Hazardous Materials* **84**(1), 29–41.

Nasrullah, M., Singh, L., Krishnan, S., Sakinah, M., Mahapatra, D. M. & Zularisam, A. W. 2020 Electrocoagulation treatment of raw palm oil mill effluent: effect of operating parameters on floc growth and structure. *Journal of Water Process Engineering* **33**, 101114.

Oliveira, A. G., Ribeiro, J. P., Abdala Neto, E. F., Lima, A. C. A., Amazonas, A. A., Silva, L. T. V. & Nascimento, R. F. 2020 Removal of natural organic matter from aqueous solutions using electrocoagulation pulsed current: optimization using response surface methodology. *Water Science & Technology* **82**(1), 56–66.

Palácio, S. M., Espinoza-Quiñones, F. R., Módenes, A. N., Oliveira, C. C., Borba, F. H. & Silva, F. G. 2009 Toxicity assessment from electro-coagulation treated-textile dye wastewaters by bioassays. *Journal of Hazardous Materials* **172**(1), 330–337.

Phalakornkule, C., Polgumhang, S., Tongdaung, W., Karakat, B. & Nuyut, T. 2010 Electrocoagulation of blue reactive, red disperse and mixed dyes, and application in treating textile effluent. *Journal of Environmental Management* **91**(4), 918–926.

Rayaroth, M. P., Aravind, U. K. & Aravindakumar, C. T. 2015 Sonochemical degradation of Coomassie Brilliant Blue: effect of frequency, power density, pH and various additives. *Chemosphere* **119**, 848–855.

R Development Core Team 2014 R: A Language and Environment for Statistical Computing. R Foundation for Statistical Computing, Vienna, Austria.

Ribeiro, J. P., Oliveira, J. T., Oliveira, A. G., Sousa, F. W., Abdala Neto, E. F., Vidal, C. B., De Keukeleire, D., Santos, A. B. & Nascimento, R. F. 2014 Treatment of sulfonated azo dye reactive red 198 by UV/$H_2O_2$. *Journal of Chemistry* **2014**, 1–11.

Rocha, A. H. Q., Oliveira, A. G., Ribeiro, J. P., Abdala Neto, E. F., Amazonas, A. A., Silva, L. T. V. & Nascimento, R. F. 2018 Application of electro-oxidation by direct and pulsed current associated to ozonation on raw water treatment. *Desalination and Water Treatment* **124**, 146–152.

Rosa, J. M., Fileti, A. M. F., Tambourgi, E. B. & Santana, J. C. C. 2015 Dyeing of cotton with reactive dyestuffs: the continuous reuse of textile wastewater effluent treated by UV/$H_2O_2$ homogeneous photocatalysis. *Journal of Cleaner Production* **90**, 60–65.

Shu, J., Liu, R., Liu, Z., Du, J. & Tao, C. 2016 Manganese recovery and ammonia nitrogen removal from simulation wastewater by pulse electrolysis. *Separation and Purification Technology* **168**, 107–113.

Verma, A. K. 2017 Treatment of textile wastewaters by electrocoagulation employing Fe-Al composite electrode. *Journal of Water Process Engineering* **20**, 168–172.

Wijannarong, S., Aroonsrimorakot, S., Thavipoke, P., Kumsopa, A. & Sangjan, S. 2013 Removal of reactive dyes from textile dyeing industrial effluent by ozonation process. *APCBEE Procedia* **5**, 279–282.

Xu, L., Huang, Q., Xu, X., Cao, G., He, C., Wang, Y. & Yang, M. 2017 Simultaneous removal of $Zn^{2+}$ and $Mn^{2+}$ ions from synthetic and real smelting wastewater using electrocoagulation process: influence of pulse current parameters and anions. *Separation and Purification Technology* **188**, 316–328.

Young, B. J., Riera, N. I., Beily, M. E., Bres, P. A., Crespo, D. C. & Ronco, A. E. 2012 Toxicity of the effluent from an anaerobic bioreactor treating cereal residues on *Lactuca sativa*. *Ecotoxicology and Environmental Safety* **76**, 182–186.

First received 5 February 2023; accepted in revised form 24 March 2023. Available online 6 April 2023